# Visible light driven photocatalysis using nitrogen doped $TiO_2$ quantum dots prepared by microemulsion route

**Yuvraj S. Malghe*, Atul B. Lavand**

*Department of Chemistry, The Institute of Science, 15, Madam Cama Road, Mumbai 400032, India*

*Corresponding author, E-mail: ymalghe@yahoo.com; Tel: (+91) 22-22844219

**Received: 31 March 2016, Revised: 22 August 2016 and Accepted: 30 November 2016**

DOI: 10.5185/amp.2017/105
www.vbripress.com/amp

## Abstract

Here, we report on microemulsion synthesis of nitrogen (N) doped $TiO_2$ quantum dots (QDs) with improved visible-light response. XRD, FTIR, XPS, EDX and Raman spectroscopy confirms that N was doped successfully in $TiO_2$ lattice. SEM and TEM study confirms spherical morphology of N-doped $TiO_2$ QDs. N-doped $TiO_2$ sample exhibit a narrower band gap and stronger visible light absorption as compared to pure $TiO_2$. The assistance of the N enhances the photocatalytic activity in the visible light region by promoting the separation of the photo generated electrons and holes to accelerate the transmission of photocurrent carrier. Photocatalytic activity study evaluated for the degradation of acifluorfen herbicide under visible-light irradiation, demonstrated that N-doped $TiO_2$ sample is more active than pure and commercial $TiO_2$. The high visible-light photocatalytic activity is attributed to the anatase crystalline phase, small crystallite size, strong visible light absorption capacity and superior electron-hole charge carrier's separation efficiency. The photoluminescence (PL) study was employed to test hydroxyl ($^{\bullet}OH$) radicals, which show that N-doped $TiO_2$ helps to produce $^{\bullet}OH$ radicals and favors to enhance its photocatalytic activity. N doped $TiO_2$ quantum dots prepared in this work exhibit better photocatalytic activity and hence having a potential to use as a photocatalyst for the degradation of harmful organic chemicals, dyes and drugs coming out from industries and will help to keep environment clean and safe. 

**Keywords:** $TiO_2$, Nitrogen doping, Visible light, photocatalysis, acifluorfen.

## Introduction

During a last decade synthesis of visible light active semiconductor photocatalysts has been a field of growing interest. Titanium dioxide ($TiO_2$) is the most widely studied heterogeneous photocatalyst due to its low cost, nontoxic nature, reusability, resistant to photo-corrosion, easy availability and high oxidative power [**1-4**]. Unfortunately, due to its large band gap (3.2 eV) $TiO_2$ is active only under UV irradiation [**5**]. Therefore, many efforts have been made to modify/shift its band gap towards the visible region. It includes non-metal doping, metal doping, dye sensitization, and semiconductor coupling [**6-11**]. Non-metal doping is regarded as one of the effectual way to enhance the visible light photocatalytic activity of $TiO_2$ [**12-15**]. Among various nonmetallic doping elements, nitrogen (N) doping has been reported to be a simple and effective way to increase the visible light absorption [**16, 17**]. So far, to dope N triethylamine, urea, thiorea, hydrazine hydrate, ammonia, EDTA etc. are used as a N source. N doped $TiO_2$ resulting from different N sources have different properties. Therefore, it is necessary to select suitable N source to integrate N into $TiO_2$ and investigate the nature of band-gap narrowing and its visible light response. It is known that N doping can cause the absorption of $TiO_2$ to visible region, but the doping mechanism is still a part of debate. Many authors state that the O atoms were substituted by N into $TiO_2$ lattice and decrease the band gap driven by mixing N 2p states with O 2p states [**18**]. It is thought that doped N forms a donor state just above the top of the valence band of anatase $TiO_2$. This process leads to the narrowing of the band gap of $TiO_2$ and create the oxygen vacancy, both of which are responsible for enhancement of visible light absorbance. Herein, we report a synthesis of N doped $TiO_2$ using a guanidine nitrate as N source. Guanidine nitrate is rich in N content (49 wt%) [**19, 20**]. Oxley et al. [**21**] has proposed possible decomposition route of guanidine nitrate, and confirmed that it dissociates to nitric acid and $NH_3$. In the present work N was doped into anatase $TiO_2$ lattice by using microemulsion route. The characteristics and properties of prepared photocatalysts were investigated by different techniques. The visible light photocatalytic activity of N-doped $TiO_2$ was studied using acifluorfen herbicide as probe molecules. The photocatalysis mechanism of N-doped $TiO_2$ was also discussed.

## Experimental

### *Materials*

Acifluorfen herbicide was obtained from Sigma Aldrich, Mumbai, India and used without any further purification. Titanium isopropoxide $Ti(iOPr)_4$ was purchased from Sigma Aldrich, Mumbai and used as a source of titanium. Cyclohexane, n-butanol, N,N,N-cetyl trimethyl ammonium bromide (CTAB), acetone, and ethanol used for the synthesis are analyticl reagent grade and were procured from SD Fine Chemicals, Mumbai and used without further purification. Commercial $TiO_2$ was procured from Loba Chemicals, Mumbai, India.

### *Synthesis of N-doped $TiO_2$*

In a typical synthesis procedure mixture containining 4g guianidine nitrate, 120 mL cylclohexane, 30 mL n-butanol and 6g N,N,N-acetyl trimethyl ammonium bromide was added in 3 mL distilled water under constant stirring. After, 18mL 1M titanium isopropoxide was added to this solution and resultant solution was stirred vigorously for 30 min. This mixture was transferred to the autoclave (with teflon-inner-liner) and kept in an oven at 150 °C for 2h. Later it was cooled to the room temperature and the residue obtained was separated using centrifugation, washed several times with distilled water followed by ethanol and finally with acetone and dried at 40 °C. The product obtained was used as a precursor. This precursor was calcined in the furnace at 500 °C for 2h to get N-doped $TiO_2$ powder. Pure $TiO_2$ was obtained using same procedure. During the synthesis of pure $TiO_2$, precursor was prepared without addition of guanidine nitrate.

### *Characterizations*

The phase identification of the samples were carried out with Rigaku (Miniflex II) powder X-ray diffractiotometer (XRD) using Cu Kα radiation (λ= 0.15405 nm) with scanning rate of $2°2\theta$ $min^{-1}$. The morphologies of the products were studied using a field-emission scanning electron microscope (SEM, ZIESS Ultra 55) and transmission electron microscope (TEM, Tecnai $G^2$, Philips). Microstructural information of the samples were examined using Jobin Yvon HR8000 UV Raman spectrophotometer (equipped with He-Ne laser excitation wavelength of 632.81 nm). X-ray photoelectron spectrum (XPS) was recorded with PHI VersaProbe-II photoelectron spectroscope (Physical Electronics, USA) with Al Kα radiation. UV–visible diffuse reflectance spectra were recorded with Shimadzu 1800 spectrophotometer furnished with an integrating sphere using $BaSO_4$ as a reference. Photoluminescence spectra of the samples were recorded with a Perkin-Elmer (LS55) photoluminescence spectrophotometer with a Xe lamp as the excitation source. The emission spectra were collected at an excitation wavelength 325 nm.

### *Experimental setup and procedure for photocatalytic degradation study*

Photocatalytic activities of pure and N-doped $TiO_2$ were investigated for the degradation of acifluorfen herbicide solution. Reaction suspension was prepared by adding 0.05g pure/ N-doped $TiO_2$ photocatalyst in 100ml acifluorfen solution (10 ppm). This aqueous suspension was stirred in the dark for 30min to attain adsorption-desorption equilibrium. Later, the solution was irradiated with visible light. The visible light irradiation was carried out in a photo reactor using a compact fluorescent lamp (65W, λ >420nm, Philips). Temperature of test solution was maintained constant throughout the experiment by circulating water around the solution. The amount of acifluorfen was monitored by sampling out 5mL aliquot solution at regular time intervals. The catalyst was first separated by centrifugation, and the concentration of acifluorfen in the supernatant solution was estimated using UV-visible spectrum recorded in the wavelength range 200-800nm.

### *Hydroxyl (˙OH) radical detection*

Terepthalic acid (TA) was used as a probe molecule to study the hydroxyl (˙OH) radicals produced after irradiating with visible light in presence of N doped $TiO_2$ quantum dots. TA acid react with ˙OH radicals, generates highly fluorescent 2-hydroxyterpthalic acid (TAOH). It shows absorption maxima at 430 nm. TA solution (0.25 mmol $L^{-1}$ ) was prepared by dissolving TA acid in NaOH solution (1.0 mmol $L^{-1}$). In this solution N doped $TiO_2$ (0.5 $gL^{-1}$) was dispersed. This mixture was irradiated with 65W compact fluorescent lamp. The solution was centrifuged and used for PL measurement.

## Results and discussion

### *XRD study*

XRD patterns of pure and N-doped $TiO_2$ prepared in the present work were recorded and are shown in **Fig. 1(a).** It can be seen that both the samples gives peaks which are marked as (101), (103), (004), (112), (200), (105), (211), (204), (110), (220), (215). All these peaks corresponds to the anatase $TiO_2$ (JCPDS card no. 21-1272). No new/additional diffraction peaks are observed in N containing $TiO_2$ . The width of the anatase crystal plane(101) peak in N-doped $TiO_2$ became broad, suggests that the crystallite size of N doped sample is smaller than pure $TiO_2$. The diffraction peak (Fig. 1a, inset) related to (101) plane of N-doped $TiO_2$ sample shifts to the lower value with respect to the diffraction peak of undoped $TiO_2$. This may be because N replaces O in $TiO_2$ structure. The shift to lower angle also implies an increase in the lattice constant due to the effective substitution of oxygen (r = 1.40 Å) by nitrogen (r = 1.71 Å) atom. It is also observed that the crystallite sizes of N-doped $TiO_2$ (7.9 nm) calculated from the diffraction data using Debye-Scherrer equation is smaller than undoped $TiO_2$ (11.5 nm).

 

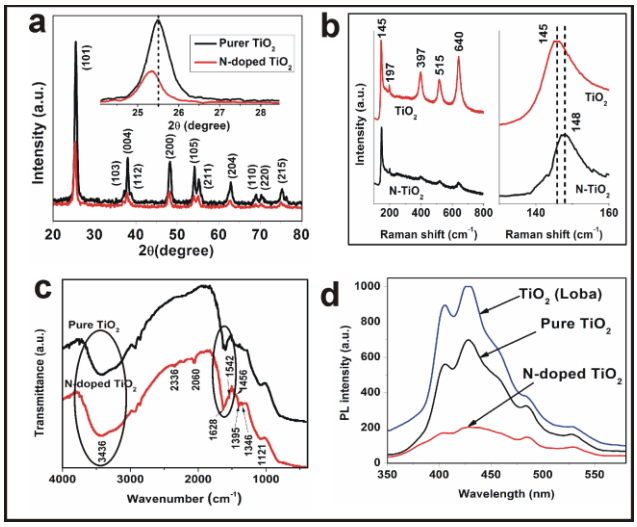


**Fig. 1. (a)** XRD patterns of pure and N-doped $TiO_2$, **(b)** Raman spectra of pure and N-doped $TiO_2$, **(c)** FTIR spectra of pure and N-doped $TiO_2$ and **(d)** PL spectra of $TiO_2$ (procured from Loba) and as synthesized pure and N-doped $TiO_2$.

### *Raman study*

**Fig. 1(b).** represents the Raman spectra of the pure and N-doped $TiO_2$ powders. Raman spectra for both the samples show peaks corresponds to the pure anatase phase, with no additional peaks due to the rutile phase, which is consistent with the XRD data. Anatase $TiO_2$ exhibit Raman bands at 145 $cm^{-1}$( Eg), 197 $cm^{-1}$ ( Eg), 397 $cm^{-1}$ (B1g), 515 $cm^{-1}$ (A1g) and 640 $cm^{-1}$ (Eg) [22]. The enlarged localized profiles shows that the Raman peaks of N-doped $TiO_2$ became broader than the pure $TiO_2$, this broadening results from smaller crystallite size of N-doped $TiO_2$. Further, a significant blue shift (toward the higher wavenumber region) is observed for N doped $TiO_2$ and the major peak is shifted from 145 to 148 $cm^{-1}$. It has been known that the shift of the peak positions and the changes of the peak width are related to changes of surface oxygen deficiency [**23, 24**].

### *FTIR study*

FT-IR spectra of as-synthesized pure and N-doped $TiO_2$ were recorded and are presented in **Fig. 1(c).** The broad band below 800 $cm^{-1}$ is ascribed to the Ti–O bond stretching vibrations [**25**]. IR bands at 2336 and 1400 $cm^{-1}$ are the characteristics of N–H stretching vibrations [**26**], which are ascribed to the N doping. The peaks at 1456 and 1121 $cm^{-1}$ corresponds to Ti-N streching. Appearance of the Ti-N bond in the sample suggests that the N species have been sucessfully incorporated in the $TiO_2$ lattice. Additionally, two major peaks located at 3436 and 1602 $cm^{-1}$ are assigned to the stretching vibration of hydroxyl group physisorbed on the surface and O–H bending of dissociated/molecularly adsorbed water molecules, respectively. The intensities of these two peaks are stronger in N-doped $TiO_2$ as compared to undoped $TiO_2$. This demonstrates that the N-doped $TiO_2$ sample is rich in surface adsorbed water and hydroxyl groups, which plays an important role in photocatalytic reaction. The hydroxyl groups captures the photo-induced holes ($h^+$) after irradiating with light, and then forms hydroxyl radicals ($^{\bullet}OH$) with high oxidation capability. Also, the surface hydroxyl group also act as absorption centers for $O_2$ molecules and finally form $^{\bullet}OH$ radicals and help to enhance the photocatalytic activity.

### *Photoluminescence (PL) study*

PL study has been widely used to investigate the efficiency of charge carrier trapping, migration, transfer, and to understand the fate of electron-hole pairs in semiconductor particles. It is known that the PL emission results from the recombination of excited electrons and holes. Thus the higher PL intensity indicates a higher recombination rate [**27–29**]. **Fig. 1(d).** shows the PL spectra of commercial $TiO_2$ and as-synthesized pure and N-doped $TiO_2$. A broad and intense photoluminescence peaks for commercial and as-synthesized undoped $TiO_2$ at 405 and 430 nm observed are attributed to the recombination of electron–hole pairs. The oxygen vacancies in pure $TiO_2$ cause the emission peaks. On the other hand N-doping increases the concentration of oxygen vacancies and the excited electrons are easily trapped by oxygen vacancies. Meanwhile, the holes are trapped by the doped N. Hence the recombination of charge carriers effectively decreased after incorporating N into $TiO_2$ lattice [**30**]. This leads to the quenching of the photoluminescence in N-doped $TiO_2$ quantum dots. So, more photogenerated charge carriers can participate in organic compound degradation, resulting in the enhancement of photocatalytic activity.

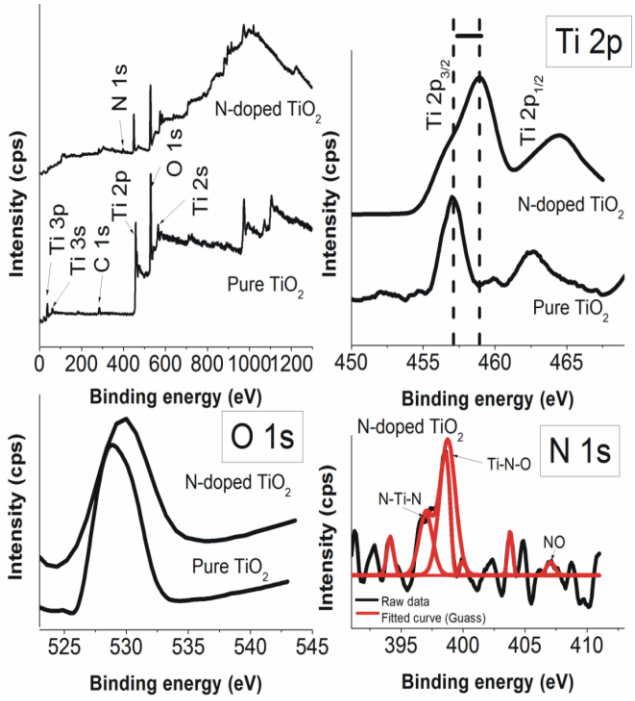


**Fig. 2.** XPS survey scan of pure and N-doped $TiO_2$ and spectra of Ti 2p, O 1s and N 1s.

***XPS study***

Surface elemental composition and electronic states of the samples were studied using XPS. XPS survey scan **(Fig. 2)** recorded for N-doped $TiO_2$ calcined at 500 °C shows the existence of Ti, O, N and C. C 1s peak is observed at 283.7 eV, which may be due to the remaining organic moiety which was not completely degraded at 500°C. N 1s peaks are located at 407.1, 398.7 and 396.1 eV. Peak at 407.1 eV could be assigned to N species bound to various surface O sites (such as NO or $NO_2$ molecules) [**31**]. N1s peak at 398.7 eV could be attributed to the N in the form of a Ti–N–O linkage, and the peak at 396.1 eV is generally recognized for the N atom replacing the O atoms in the $TiO_2$ crystal lattice to form N–Ti–N bond [**32**]. The relative atomic concentrations of N in the N-doped $TiO_2$ sample is found to be 3.4 at.% (XPS data). Ti 2p XPS spectrum shows two peaks at 462.8 and 457.1 eV, which are assigned to the Ti $2p_{1/2}$ and Ti $2p_{3/2}$ states, respectively. N doped $TiO_2$ sample shows shift in the Ti 2p peaks towards higher binding energy as compared to pure $TiO_2$. Binding energies of O1s are located at 528.7 and 530.5 eV for pure and N-doped $TiO_2$. O1s peak is wide and asymmetric, demonstrating that there must minimum two kinds of O species exist from 525 to 535 eV. It includes crystal lattice O and chemiadsorbed O. The crystal lattice O peak is mainly attributed to the contribution of Ti–O bond in $TiO_2$ crystal lattice, while the chemiadsorbed O peak is closely related to the hydroxyl groups (OH) resulting mainly from the chemisorbed water. As expected, the content of hydroxyl O in N doped $TiO_2$ sample increased remarkably in contrast to that of pure $TiO_2$, which indicates that doping with N made the catalyst possessing more hydroxyl groups, which favors not only the trapping of electrons to enhance the separation efficiency of electron/hole pair but also forming the surface free radical to enhance the photocatalytic degradation of pollutants.

***SEM and TEM study***

The surface morphology and size of the N-doped $TiO_2$ QDs synthesized in the present work were studied using FE-SEM and TEM techniques. **Fig. 3(a)** represents the FE-SEM image of as synthesized N-doped $TiO_2$ QDs. From FE-SEM image, it is observed that the N-doped $TiO_2$ QDs are spherical in shape and they are tightly bound in spheres. Further the chemical composition of the N-doped $TiO_2$ QDs was obtained using EDS spectrum (**Fig. 3(b)).** EDS spectrum show that N-doped $TiO_2$ QDs consist Ti, N and O. TEM image (**Fig. 3(c))** of N-doped $TiO_2$ clearly shows that particles are fine, spherical and homogeneously distributed. From the TEM image, the particle size of the N-doped $TiO_2$ QDs was studied. It indicate that the size of the N-doped $TiO_2$ QDs varies between 5 to 8 nm. The selected area electron diffraction (SAED) pattern **(Fig. 3(d))** illustrates that there are several electron diffraction rings. The d-spacings of the rings corresponding to the hkl planes (101), (103), (200) and (105) were identified. These hkl planes are matches with pure anatase phase of $TiO_2$ having tetragonal structure.

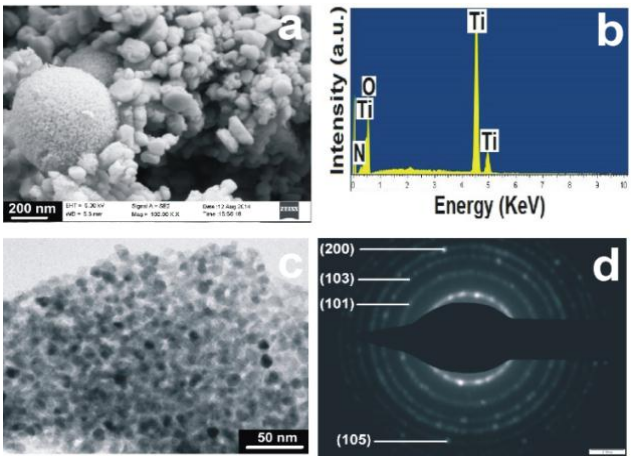


**Fig. 3. (a)** SEM image, **(b)** EDS spectrum, **(c)** TEM image and **(d)** SAED pattern of N-doped $TiO_2$ QDs.

***UV– visible diffuse reflectance spectroscopic study***

The coloration of the modified catalyst is in good agreement with bathochromic shift observed in its spectra, recorded using diffuse reflectance (DRUV) spectroscopy technique. In general speaking, the narrower is the band gap energy of the semiconductor, the higher is its photocatalytic activity. The diffuse reflectance spectra of commercial $TiO_2$, pure $TiO_2$, and N-doped $TiO_2$ are shown in **Fig. 4**.

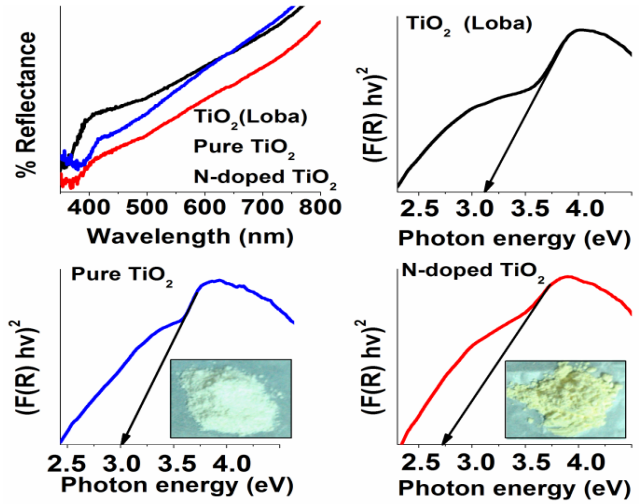


**Fig. 4.** Diffuse reflectance spectra and Kubelka-Munk plots for $TiO_2$ procured from Loba and as synthesized pure and N-doped $TiO_2$.

Band gap energies of these samples were calculated according to the Kubelka–Munk function [**33**]. It is observed that commercial $TiO_2$ and undoped $TiO_2$ exhibits the band gap energies 3.16 and 3.01 eV respectively. The absorbance edge of N doped $TiO_2$ sample is markebly shifted to the visible light region, demonstrating the decrease in the band gap energy. N doping is responsible for the formation of new energy level (localized N 2p states) in the band gap of $TiO_2$. After calculation, the band gap energy of N doped $TiO_2$ is found to be 2.71 eV. As a result, the N doped $TiO_2$ should

 

most probably possess excellent visible light photocatalytic activity for degradation of organic compounds.

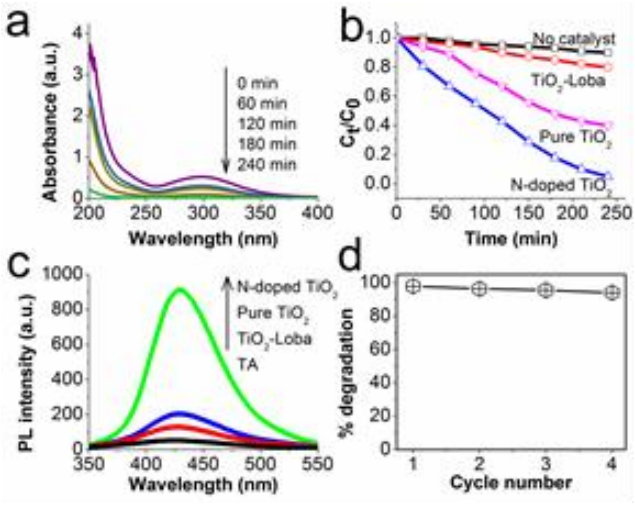


**Fig. 5(a)** UV-vis spectra of acifluorfen herbicide solution after visible light irradiation for different times intervals in presence of N-doped $TiO_2$, **(b)**Visible light photocatalytic degradation of acifluorfen solution using commercial $TiO_2$, pure and N-doped $TiO_2$ prepared in the present work (Reaction conditions: $C_0$ = 10 ppm, Catalyst loading: 1g $L^{-1}$) **(c)**Fluorescence spectra of Terepthalic acid (TA) in presence of $TiO_2$ (Loba), pure $TiO_2$, N-doped $TiO_2$ and **(d)** Reuse of N-doped $TiO_2$ photocatalyst upto fourth cycle.

### *Photocatalytic activity study*

The degradation of acifluorfen herbicide was studied to evaluate the photocatalytic activity of as-synthesized N-doped $TiO_2$ and the results are shown in **Fig. 5(a)**. The photocatalytic activity of commercial $TiO_2$ sample (proceured from Loba Chemicals Ltd.) was also measured as a reference. The experimental results shows that in absence of the photocatalyst the acifluorfene concentration changes a little after irradiating for 4h. Noticeably, as shown in **Fig. 5(b)**, the photocatalytic activity of $TiO_2$ nanoparticles is greatly improved by N doping, which is in good agreement with the above XRD, DRS, PL and FT-IR results. Based on the above discussions, the enhanced photocatalytic activity of N doped $TiO_2$ is attributed to the small crystallite size, well anatase crystallinity, narrow band gap, intense light absorbance in visible region, high separation rates of photogenerated charge carriers and more content of surface hydroxyl groups. **Fig. 5(c**) shows PL spectra of Terepthalic acid (TA) solution exposed to visible light for 4 h, in presence of different photocatalysts. The blank experiment result indicates that in absence of catalyst no signal generated at 429 nm. As compared to pure $TiO_2$, PL intensity for N-doped $TiO_2$ increases noticeably with irradiation time. This reveals the generation of $^{\bullet}OH$ radicals which are responsible for degradation of acifluorfen. Furthermore, even after fourth cycle it is still able to achieve 94% degradation of acifluorfen, which implies excellent stability of N-doped $TiO_2$ **(Fig. 5(d))**. The high visible-light photocatalytic activity and excellent photochemical stability suggest that the as synthesized N-doped $TiO_2$ QDs may use as promising photocatalyst for removing acifluorfen herbicide from waste water.

### *Mechanism view for visible light-induced photoactivity in N-doped $TiO_2$ QD's*

On the basis of above results we have proposed the mechanism of visible light-induced photocatalytic activity of the N-doped $TiO_2$ QD's, as illustrated in **Fig. 6**. The band gap of pure $TiO_2$ is 3.01 eV and could be excited with light having wavelength less than 411 nm.

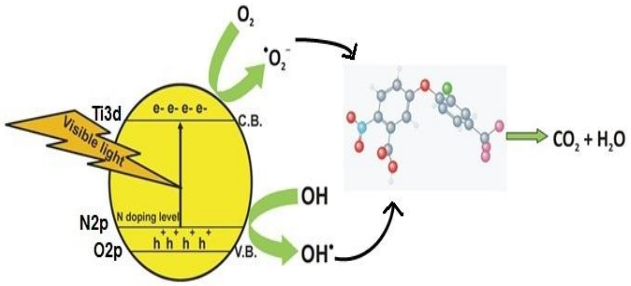


**Fig. 6.** Proposed reaction mechanism for the visible light photocatalytic degradation of acifluorfen herbicide using N-doped $TiO_2$ QD's

N doping into the crystal lattice of $TiO_2$ modifies the electronic band structure of $TiO_2$ and leads to a new substitution of N 2p band, above O 2p valance band, which decreases the band gap of $TiO_2$ and shifts optical absorption to the visible light region. Due to N doping, the separation rates of photogenerated charge improves, which favours the enhancemnet of photocatalytic activity. The visible light induced photocatalytic degradation of acifluorfene herbicide is proposed as follows,

$$N\text{–}TiO_2 + hv \text{ (visible light)} \rightarrow h^+_{(VB)}\ TiO_2 + e^-_{(CB)}\ TiO_2$$

After, the reactive photogenerated holes react with $OH^-$ adsorbed on the catalyst surface form hydroxyl ($OH^{\bullet}$) radicals, meanwhile the excited electrons in the conduction band moves towards the surface and interact their with surface-adsorbed oxygen produces superoxide anion radicals ($^{\bullet}O_2-$), which reacts with $H_2O$ and forms $OH^{\bullet}$ radicals, the most powerful oxidizing species.

$$h^+_{(VB)} + OH^- \rightarrow OH^{\bullet}$$
$$O_2 + e^-_{(CB)} \rightarrow {}^{\bullet}O_2-$$
$$O_2^{\bullet}- + H_2O \rightarrow OH^{\bullet} + OH^-$$
$$OH^{\bullet} + {}^{\bullet}O_2- + \text{acifluorfene} \rightarrow \text{Intermediates} \rightarrow CO_2 + H_2O$$

The hydroxyl groups plays an important role in inhibiting the recombination rate of photogenerated electron and hole pairs. From PL and FTIR study it was revealed that N doped $TiO_2$ produces a large number of hydroxyl groups and exhibit higher photocatalytic activity.

 

## Conclusion

N-doped $TiO_2$ QD's were prepared using microemulsion method. Guanidine nitrate is used as a N source to dope N into $TiO_2$ lattice successfully. Raman and XPS study reveals that N in $TiO_2$ has the chemical environment as N-Ti-O and Ti-O-N. N doping in $TiO_2$ lattice leads to the shifting of strong optical absorption towards visible region, enhancement in the photo generated electron-hole pairs and increase in content of surface hydroxyl groups. N-doped $TiO_2$ QDs synthesized in present work exhibit excellent visible light photocatalytic activity (for degradation of acifluorfen) as compared to commercial and un-doped $TiO_2$. The catalyst showed 94% degradation, even after 4 cycles of repetitive use, indicating the promising recyclability and photochemical stability of N-doped $TiO_2$ QDs.

**Acknowledgements**

Authors are thankful to SAIF, IIT, Mumbai for recording the FE-SEM and TEM images of samples. One of the authors, Atul B. Lavand is grateful to UGC, New Delhi, India for providing BSR-Research fellowship.

**Author's Contribution**

AB - Performed the experiments, YS - Data analysis, Wrote the paper. Authors have no competing financial interests.

**References**

1. Imani, R.; Pazoki, M.; Tiwari, A.; Boschloo, G.; Turner, APF.; Kralj-Iglic, V.; Iglic, A.; Nanoscale, **2015**, *7*, 10438.
2. Yang, H. G.;Sun, C. H.;Qiao, S. Z.;Zou, J.;Liu, G.; Smith, S. C.;Cheng, H. M.; Lu, G. Q. *Nature*, **2008**, *453*, 638.
3. Buonsanti, R.; Grillo, V.; Carlino, E.;Giannini, C.;Kipp, T.;Cingolani, R.;Cozzoli,P.D. *J. Am. Chem. Soc*., **2008**, *130*, 11223.
4. Patra, H. K.; Imani, R.; Jangamreddy, J. R.; Pazoki, M.; Iglic, A.; Turner, APF.; Tiwari, A.; Scientific Reports, **2015**, *5*, 14571.
5. Bosc, F.; Ayral, A.; Albouy,P. A.; Guizard,C, *Chem. Mater*., **2003**, *15*, 2463.
6. Sobana, N.; Elvam, K.; Swaminathan,M. *Sep. Purif. Technol*., **2008**, *62*, 648.
7. Song,S.;Tu,J.;Xu,L.;Xu,X.;He, Z.;Qiu,J. *Chemosphere*, **2008**, *73*, 1401.
8. Shukla, S. K.; Bharadvaja, A.; Parashar, G. K.; Mishra, A. P.; Dubey, G. C.; Tiwari, A.; Advanced Materials Letters, **2012**, 3, 365.
9. Mahyar,A.;Behnajady, M. A.;Modirshahla,N. *Ind. J. Chem. A*, **2010,** *49*, 1593.
10. Batista,A. P. L.;Carvalho,H. W. P.;Luz, G. H. P.;Martins,P. F. Q.;Goncalves, M.; L. Oliveira,C. A. *Environ. Chem. Lett*., **2010**, *8*, 63.
11. Bansal,P.;Dhir,A.;Prakash,N. T.;Sud, D. *Ind. J. Chem. A*, **2011**, *50*, 991.
12. Asahi, R.; Morikawa, T.; Ohwaki,T.;Aoki, K.;Taga,Y. *Science*, **2001**, *293*, 269.
13. Sakthivel, S.;Kisch, H. *Angew Chem.*,**2003**, *42*, 4908.
14. Li, Q.; Doped titanium oxide photocatalysts: Preparation, structure and interaction with viruses, ProQuest, 2007.
15. Yamaki,T.;Umebayashi,T.;Sumita,T.;Yamamoto,S.;Maekawa, M.;Kawasuso,A.; Itoh,H. *Nuclear Instruments and Methods in Physics Research Sect. B*, **2003**, *206*, 254.
16. Moriya, Y.;Takata,T.;Domen,K.;Coord. *Chem. Rev.*, **2013**, *257*, 1957.
17. Xiang,Q.;Yu,J.;Wang W.;Jaroniec, M. *Chem. Commun*. **2011**, *47*, 6906.
18. Liu,G.;Yang,H. G.;Wang,X;Cheng, L.;Pan,J.;Lu, G. Q.;Cheng,H. M. *J. Am. Chem. Soc*. **2009**, *131*, 12868.
19. Mendenhall,I. V.; Smith,R. G.; CN *Patent 03812220*, **2003.**
20. Ulas,A.;Risha,G. A.;Kuo,K. K. *Fuel*, **2006**, *85*, 1979.
21. Oxley,J.;Smith, J.;Naik,S.;Moran,J. *J. Energ. Mater*. **2008**, *27*, 17.
22. Yu,Y.;Yu,J.C.;Yu,J.;Kwok,Y. C.;Ding, L.;Ge, W.;Che, Y.;Zhao,J.;Wong, P. K. *Appl. Catal. A: Gen.* **2005**, *289*, 186.
23. Wu,Y.;Zhang, J.;Xiao,L.;Chen, F. *Appl. Catal. B: Environ.* **2009**, *88*, 525.
24. Nassoko,D.;Li, Y-F.;Wang,H.;Li, J-L.;Li, Y-Z.;Yu, Y. *J. Alloys Comp*. **2012**, *540*, 228.
25. Yu,J. G.;Yu,H. G.;Cheng,B.;Zhao,X. J.;Yu, J. C.;Ho,W. K. *J. Phys. Chem. B*, **2003**, *107*, 13871.
26. Silverstein, R. M.;Bassler, G. C.;Morrill, T. C. *Spectrometric Identification of Organic Compounds, 4th ed., New York: John Wiley & Sons*, **1981**.
27. Yang,M. J.;Hume,C.;Lee,S;Son Y. H.;, Lee, J. K. *J. Phys. Chem. C.* **2010**, *114*, 15292.
28. Xin,B.;Jing,L.;Ren,Z. .;Wang,B.;Fu, H. *J. Phys. Chem. B.* **2005**, *109*, 2805.
29. Li,Y. F.;Xu,D.;Oh,J. H.;Shen,W.;Li, X.;Yu,Y. *ACS Catal*. **2012**, *2*, 391.
30. Fang,X.;Zhang,Z.;Chen, Q.;Ji, H.;Gao,X. *J. Solid State Chem.* **2007**, *180*, 1325.
31. Ananpattarachai, J.;Kajitvichyanukul,P.;Seraphin, S. *J. Hazard. Mater*. **2009**, *168*, 253.
32. Sheng,Y.;Xu, Y.;Jiang,D.;Liang, L.;Wu, D.;Sun, Y. *Int. J. Photoenergy.* **2008**, 1.
33. Bai, Y-Y.;Lu,Y.;Liu,J-K. *J. Hazard. Mater*.**2016**, *307*, 26.

 